PRELIMINARY TEST OF A NOZZLE TYPE PLASMA EXPANSION CUP

M. Kobayashi, A. Takagi, S. Fukumoto
National Laboratory for High Energy Physics
Oho-machi, Tsukuba-gun, Ibaraki, Japan

and

Th. J.M. Sluyters
Brookhaven National Laboratory
Upton, New York, U.S.A.

Abstract

A nozzle-type plasma expansion cup having the throat aperture of 1.3 mmϕ was tested in order to improve the intensity and the emittance of the duoplasmatron beam. The maximum ion current was 800 mA at 60 keV with a normalized emittance of 0.35 cm·mrad. The high current at a relatively low arc current and low pressure indicates the nozzle-type plasma cup being promising. The observed aberration is discussed in relation to the plasma boundary distortion.

Introduction

Most of the operational proton sources for the high energy accelerators are the duoplasmatrons with a plasma expansion cup. So far, the increase in current up to a few amperes has been rather successful by using a plasma cup having a large exit diameter and a large anode hole. The emittance, however, also increases with the current and the brightness figure has a trend of decrease. Consequently, production of a dense plasma and transport of the plasma to the exit of the expansion cup will be main problems to be solved.

Recently, Kovarik and Sluyters[1] analyzed, by taking the duoplasmatron of BNL as an example, the physical phenomena in the expansion cup; the pressure gradient, ionization, plasma density and collisions. They have shown that the extracted ion beam comes from two plasmas of different origins; the primary plasma that is produced inside the discharge chamber and the secondary plasma that is produced around the entrance and upstream part of the cup. A significant part of the ion beam is due to the secondary plasma. A characteristic feature of the ion produced in the secondary plasma is the low kinetic energy and the nearly isotropic velocity distribution. Near the entrance in the expansion cup, where the pressure is still not so low, the mean free path of the ion-ion, ion-electron, electron-electron, ion-molecule and electron-molecule collision is smaller than or as small as the physical dimension of the cup. Consequently, the plasma flow may be approximated by a continuous flow of compressible fluid. The proper transport of the plasma may then be successful by the use of a supersonic nozzle geometry for the expansion cup. The proposal of Kovarik and Sluyters for the nozzle type expansion cup was the first analytical approach for designing the expansion cup.

In order to examine the prediction of Kovarik and Sluyters, we have tested a nozzle-type plasma expansion cup. the preliminary result of which is presented here.

Experiment

In Fig.1 is presented a sketch of the experimental arrangement.

The duoplasmatron[2] was mounted on a test stand insulated from the ground by more than several tens of kilovolts. Two types of cathode were used: a Th-W wire of 0.5 mm in diameter and a carburized Th-W wire of 0.8 mm in diameter. The snout channel is 5 mm in diameter and 5 mm in length. The duoplasmatron was operated with the pulse width of 50 μsec at a repetition rate of 5 pps. The source gas pressure was measured by a Pirani gauge calibrated to the air.

A nozzle-type plasma expansion cup (Fig.2) was designed for the ion current of 300 mA with the current density of about 100 mA/cm^2 at the exit. For ease of machining, the inner profile of the cross section consists of a circle and straight lines: a circle of 2.4 mm in the radius and three straight lines with the angles to the axis of 37°55', 24°30' and 12°. The distance between the snout and the nozzle's throat is 7.8 mm. The throat aperture is 1.3 mm and the exit of the cup 22 mm in diameter. The cup was aligned concentric to the snout within an accuracy of 0.2 mm.

The extractor electrode (of stainless steel) has an aperture of 20 mm with a geometry similar to the Pierce one. It was aligned to the anode of the ion source with an accuracy better than 0.1 mm. The distance of the extraction electrode from the exit of the expansion cup, L_{ext} (indicated in Fig.2), is adjustable with an accuracy of 0.05 mm without breaking the vacuum.

The ion current was obtained through a 50 Ω resistor by collecting the total current flowing into the slit system, which was located at L_s = 37.5 mm downstream of the extractor. The biassing negative voltage above several kilovolts was applied between the extraction electrode and the slits in order to suppress the secondary electrons.

The beam emittance was obtained from a polaroid photograph of the slit images on an aluminized quartz plate, which was located at a distance of 100 mm from the slit. A slit plane has one-dimensional parallel slits of 0.2 mm spacing at intervals of 5 mm. The photograph was taken with the size of the object.

The electrical connections to the ion source, the extractor electrode and the measuring slit system are shown in Fig.3.

Intensity

Typical dependences of the ion current (I^+) on

the arc current (I_a), the magnet current (I_m), and the extraction voltage (V_{ext}) are presented in Figs. 4∼6 respectively. Because the extractor is biassed by V_b with respect to the measuring slits placed at the ground level, V_{ext} is equal to the high voltage applied to the extractor (H.V.) minus V_b. The energy of the beam measured, however, is given not by V_{ext} but by H.V..

The maximum ion current of 800 mA was obtained at 60 keV for I_a = 30A, V_a = 180V, I_m = -4.6A (the peak field ≃ 3.5 kG), the source gas pressure p = 0.13 Torr and L_{ext} = 13.0 mm. In order to check the accurate measurement of the ion current, the saturation of I^+ with respect to V_b was confirmed as in Fig. 7. V_b as high as -6 kV (-7 kV) was necessary for 300 mA (800 mA) beam.

The extracted ion current density of 255 mA/cm^2 obtained for the 800 mA beam was roughly half of the space charge limited current density of 560 mA/cm^2, calculated for a parallel dipole approximation. It is, however, much higher than the designed value.

Emittance

A typical photograph of the slit images is presented in Fig.8 for a 420 mA, 55 keV beam. The emittance plot is given in Fig.9. The emittance pattern has a marked shape[3] of the central part plus two wings. The normalized emittance (= Area·βγ/π) is 0.20 cm·mrad corresponding to the brightness figure of 2.1 x 10^{10} A/m^{2}rad^2.

For different levels of the ion current with the different parameters of the discharge, the emittance pattern has nearly the same feature, i.e. the central narrow part plus the two wings (Fig.10). What is the cause of this strong aberration? The aberration will be caused either by the plasma boundary and (or) the extractor. The fact that the aberration hardly depends on either of the extraction voltage, the extractor position and the ion current (i.e. the beam size) indicates that the aberrations would mainly be due to the plasma boundary distortion.

In Fig.11 is shown the beam optics for the 420 mA, 55 keV beam. The beam trajectory was traced back from the slit images through the slits up to the plasma cup. There exist clearly two different ion emitting regions; the one at the centre of the cup and the other at the vicinity of the plasma boundary. A possible plasma boundary, though not measured, is also indicated. The central hill is roughly created by the directional ions which originate from the primary plasma. The ions produced from the secondary plasma in the plasma cup expand isentropically and form a broad plasma boundary around the central hill. The plasma boundary for the ions originating from the primary plasma will be predominantly determined by the density and the ion energy of the primary plasma, while those from the secondary plasma will depend significantly on the geometries of the extractor and the contour of the exit of the plasma cup. For low intensity beams, the central hill may be reduced and the plasma boundary may be such as a dotted curve indicated in Fig.11.

Typical beam parameters obtained are listed in Table I. For the ion current of 100∼800 mA at several tens of keV, the normalized emittance (E_n) slowly increases from 0.12 to 0.35. The brightness figure lies between (1.6 ∼ 2.4) x 10^{10} A/(m·rad)^2. It is roughly constant (Fig.12), though not thoroughly studied, indicating the dependence of $E_n \propto (I^+)^{1/2}$ in agreement with the Steenbergen's speculation[4].

Conclusion

At the present stage of the tests, the nozzle-type plasma cup is promising (Fig.12) because a rather high ion current of 800 mA was obtained for a relatively low arc current of 30 A and low source pressure of 0.13 Torr, and because the brightness figure is as large as 2 x 10^{10} A/(m·rad)^2 in spite of the aberrated emittance pattern.

The aberration is not necessarily a negative proof against the advantage of the nozzle-type plasma cup. The advantages expected for the nozzle-type plasma cup, are the reduction of the loss of the primary plasma to the walls during the transport and the isentropic expansion of the secondary plasma (and probably also a part of the primary plasma). These, however, will hold only at the vicinity of the nozzle throat, because the source pressure in the present experiment is only 0.1∼0.2 Torr instead of 0.5 Torr assumed by Kovarik and Sluyters[1] in their original work. After passing through the nozzle at a distance of several mm's, the validity of a continuous fluid flow approximation to the plasma becomes unfavourable and is finally improper near the exit of the cup. Consequently, the extraction geometry is an important factor for proper shaping of the plasma boundary surface at the exit of the cup, regardless whether or not the approximation of a continuous flow is valid at the entrance and upstream part of the cup. Optimization of the extraction geometry remains to be studied to produce a flat plasma boundary.

Acknowledgments

The authors are grateful to Professor T. Nishikawa for illuminating discussions and continuous encouragements.

They are also indebted to Messrs. T. Ikeda and Y. Fukuda of Tokyo Precision Instruments Co. for the construction of the precision mechanical parts and to Messrs. H. Kimura and K. Ishigaki of Japan Atomic Co. for the supply of the carburized Th-W cathodes.

References

1) V. Kovarik and Th. Sluyters: "An analytical Approach to the Design of a Plasma Expansion Cup" Proc. Symposium on Ion Sources and Formation of Ion Beam, BNL, 1971, p.21

2) S. Fukumoto, S. Inagaki, M. Kobayashi, T. Nishikawa and S. Takami: "Preliminary Study of Ion Source and High Gradient Column" ibid, p.121

3) A similar type of aberration was observed by A. Delbarre, J. Faure and R. Vienet: "An Ion Source with a Large Brightness" Fifth Intern. Conf. High Energy Accelerators, Frascati, p.147

4) A. Van Steenbergen: IEEE Trans. Nucl. Sci. NS-12, No.3 (1965) 746

Table I

Typical beam parameters of the present ion source (L_{ext} = 13 mm)

Beam Current I^+	Arc Current I_a	Arc Voltage V_a	Magnet Current I_m	Source Pressure P	Ion Energy T	Phase Space Area A	Normalized Emittance $E_n = \frac{A\beta\gamma}{\pi}$	Brightness $B = \frac{2I^+}{\pi^2 E_n^2}$
mA	A	V	A	Torr	keV	cm·mrad	cm·mrad	A/m^2rad^2
100	20	120	+ 2.8	0.07	48	38	0.12	1.6×10^{10}
200	20	120	+ 3.0	0.08	48	40	0.14	2.3×10^{10}
330	29	180	- 1.4	0.13	64	55	0.18	2.1×10^{10}
430	29	180	- 1.9	0.13	64	70	0.23	1.6×10^{10}
420	36	160	+ 1.9	0.19	55	59	0.20	2.1×10^{10}
700	32	180	- 3.9	0.13	55	73	0.24	2.4×10^{10}
800	30	180	- 4.6	0.13	60	111	0.35	1.6×10^{10}

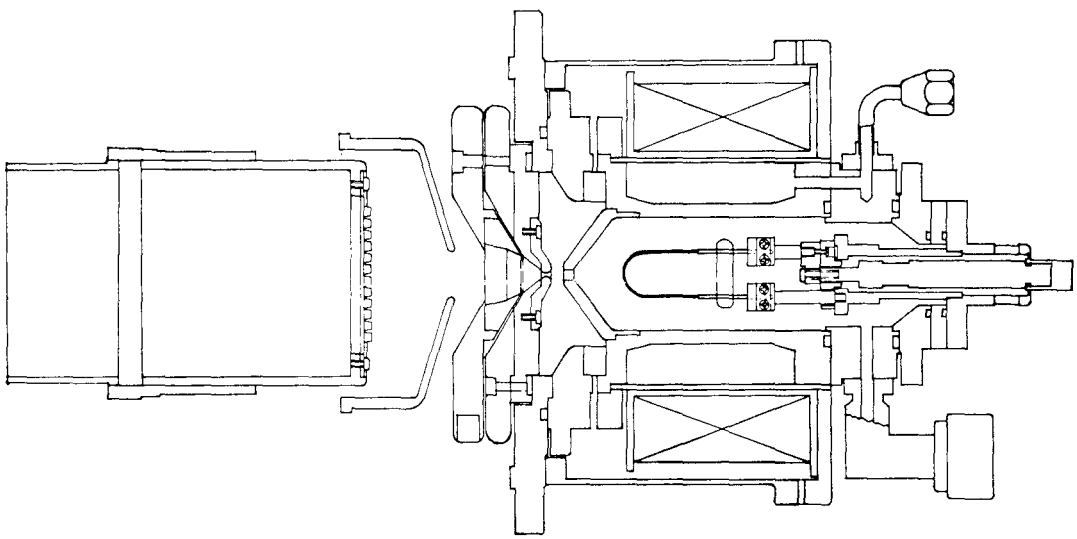

Fig.1. A sketch of the experimental arrangement.

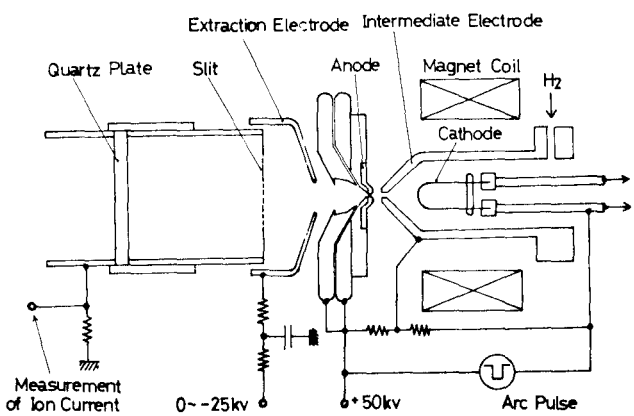

Fig.2. The tested expansion cup.

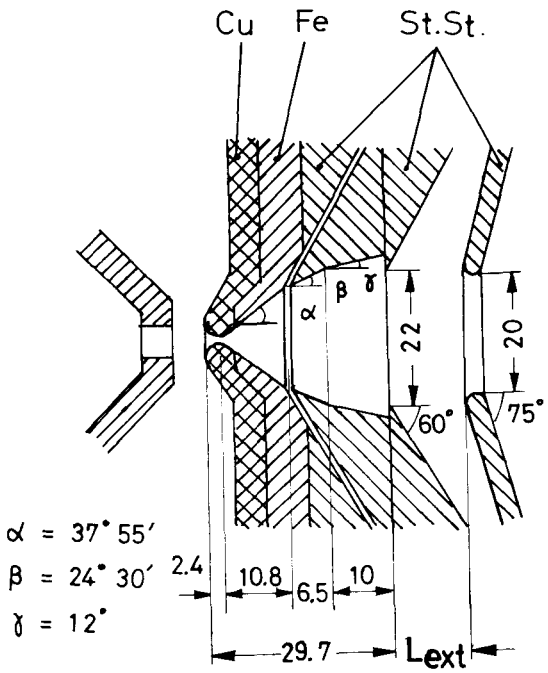

Fig. 3. The electrical connections.

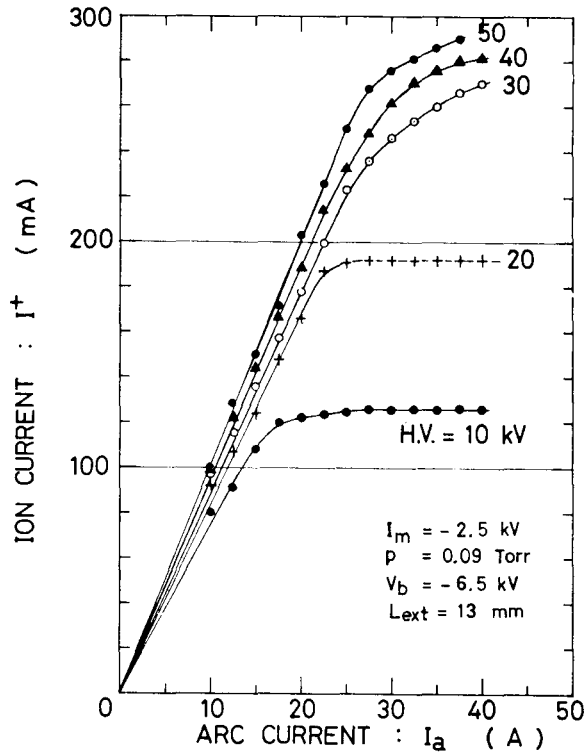

Fig. 4. The ion beam current vs. the arc current for various fixed extraction voltages. The cathode was carburized Th-W wire.

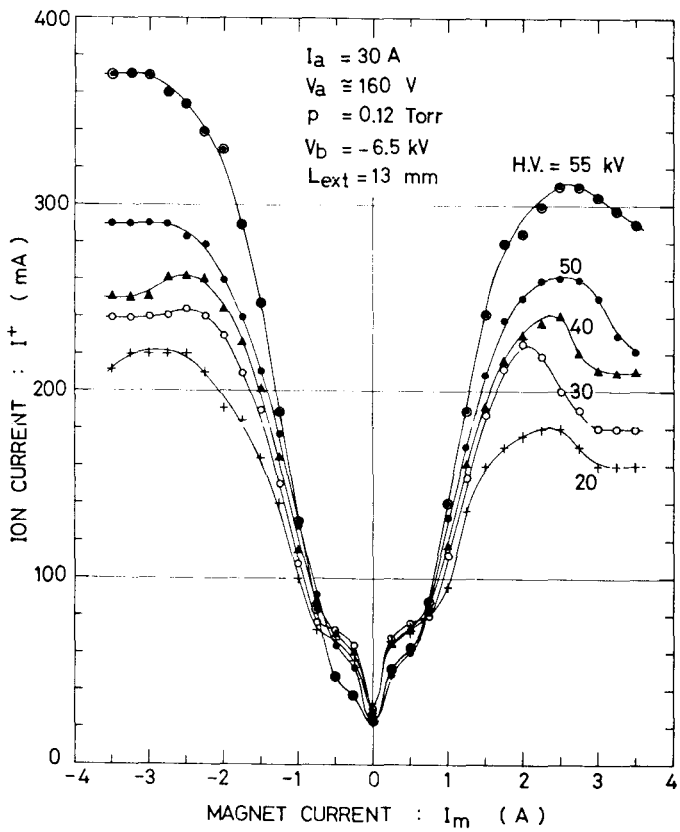

Fig. 5. The ion beam current vs. the magnet current for various fixed extraction voltages.

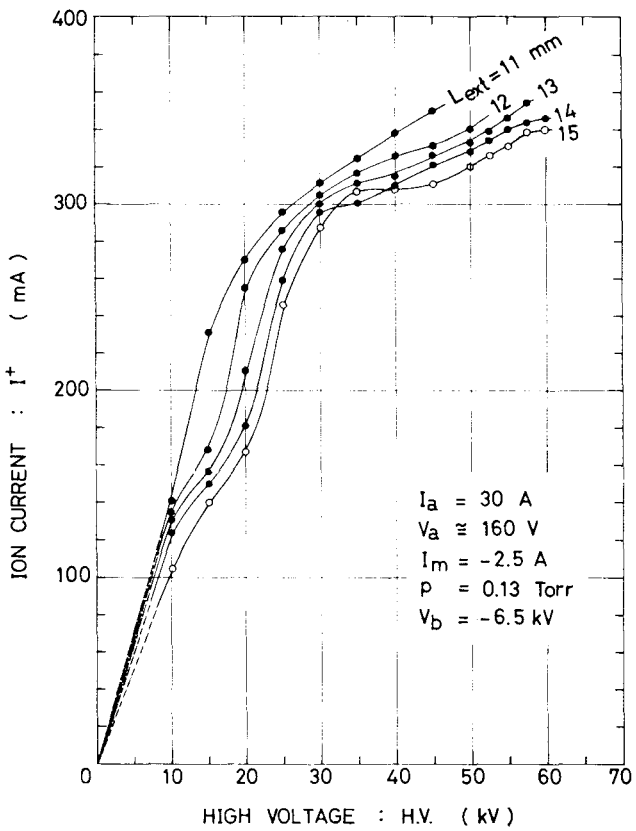

Fig. 6. The ion beam current vs. the high voltage for various positions of the extractor.

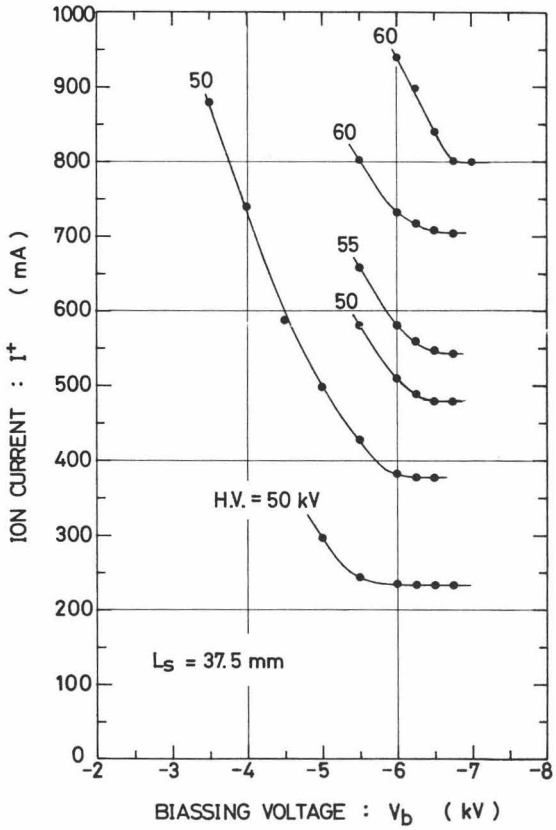

Fig. 7 The effect of V_b on the measured value of the ion current. Parameters of the arc discharge was varied. The cathode was a Th-W wire 0.5 mm diam.

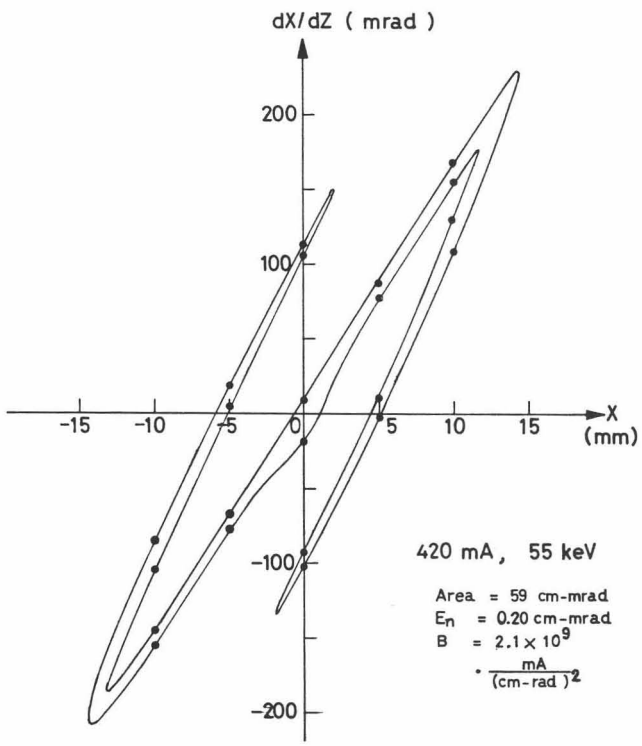

Fig. 9. The emittance pattern for the 420 mA, 55 keV beam of Fig. 8.

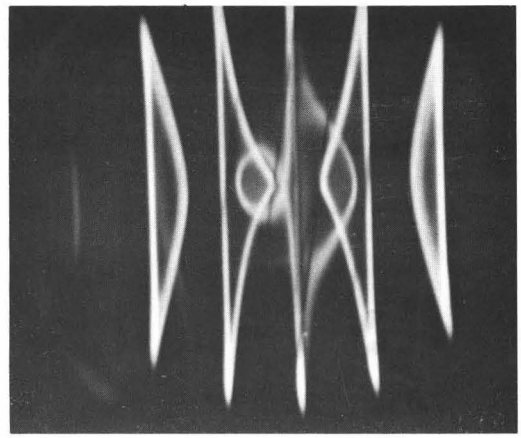

Fig. 8. Slit images for a 420 mA, 55 keV beam (see Table I).

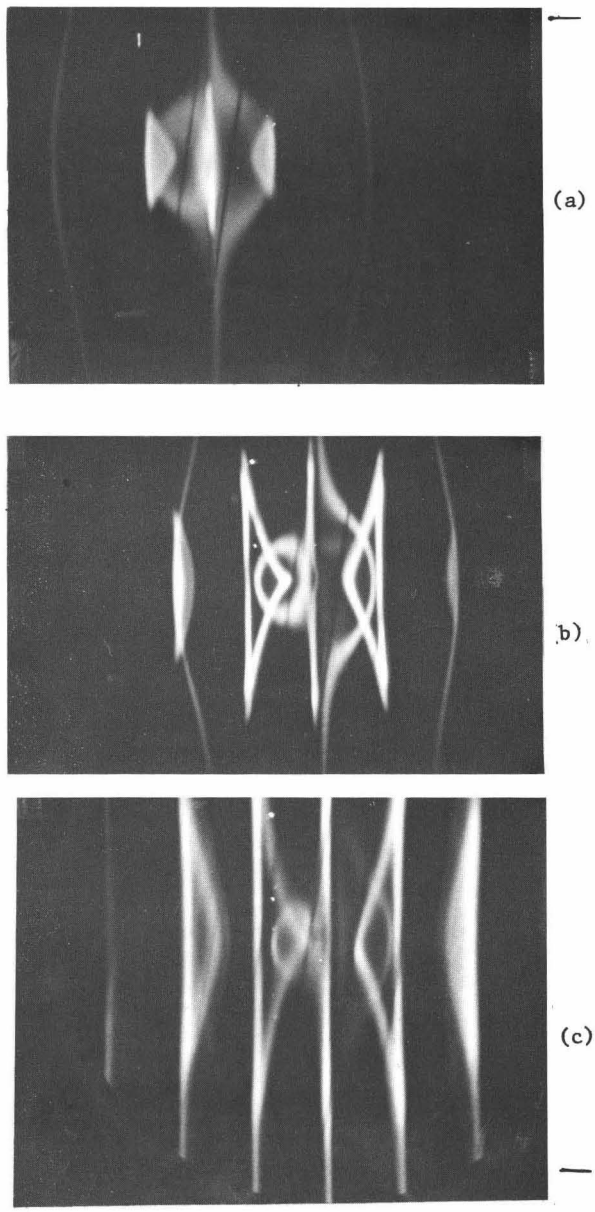

Fig. 10. Typical slit images for (a) 45 mA, 45 keV beam; (b) 350 mA, 62 keV beam; and (c) 800 mA, 60 keV beam (see Table I).

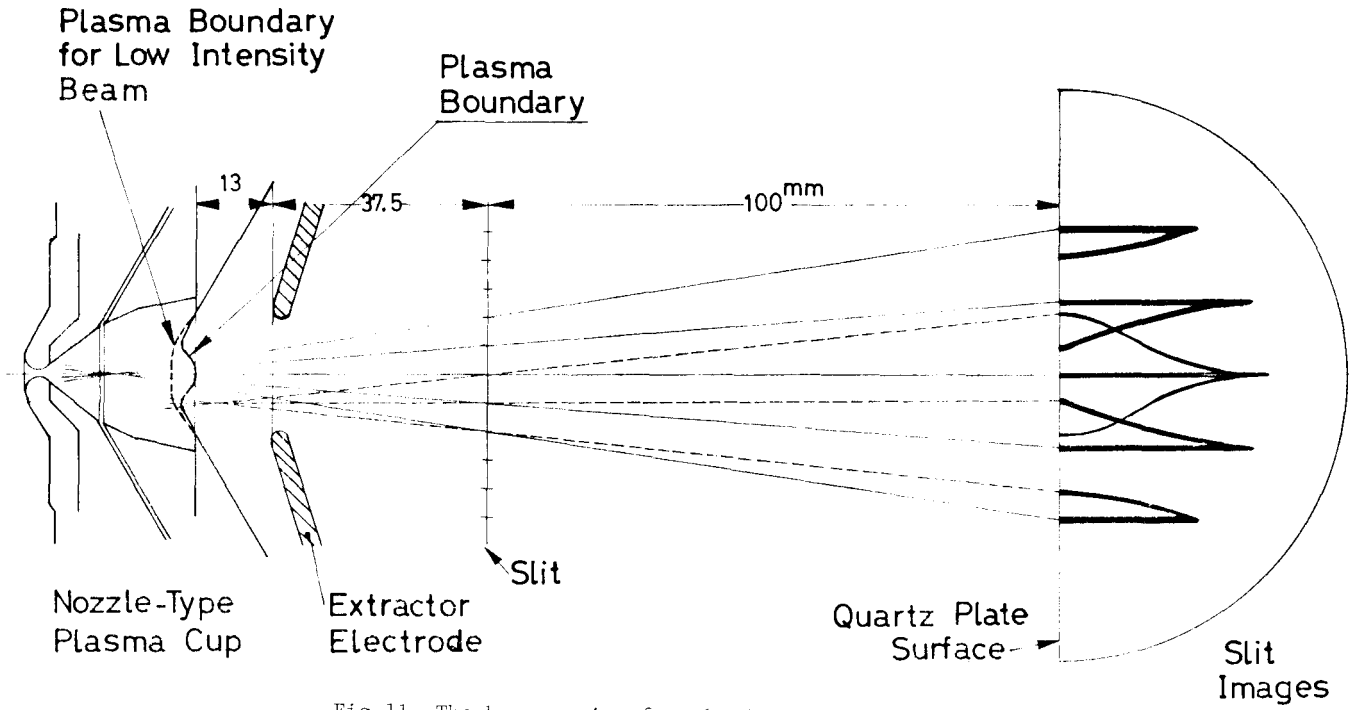

Fig.11. The beam optics for the 420 mA beam of Fig.6.

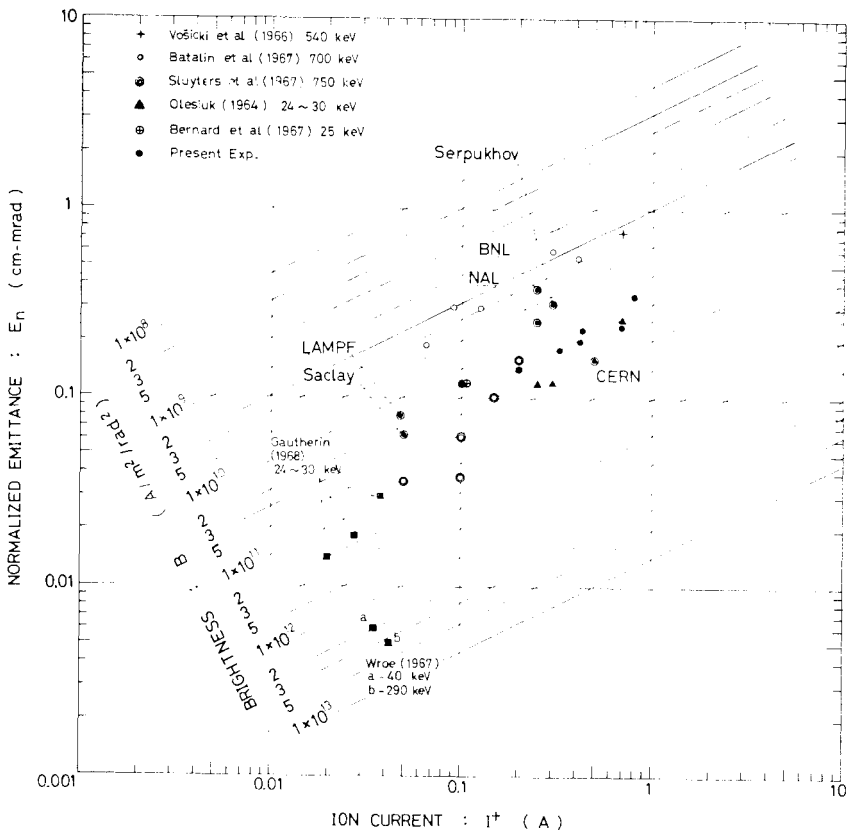

Fig.12. Comparison of some of the beam parameters for duoplasmatrons. Double circles show the beam parameters of the operational ion sources for high energy accelerators in 1971. The present data are indicated by solid circles.